# Performance mapping of the R744 ejectors for refrigeration and air conditioning supermarket application: a hybrid reduced-order model

Michal Haida[a,*], Jacek Smolka[a], Armin Hafner[b], Ziemowit Ostrowski[a], Michał Palacz[a], Kenneth B. Madsen[c], Sven Försterling[d], Andrzej J. Nowak[a], Krzysztof Banasiak[e]

[a] *Institute of Thermal Technology, Silesian University of Technology, Konarskiego 22, 44-100 Gliwice, Poland*
[b] *NTNU Department of Energy and Process Engineering, Kolbjørn Hejes vei 1d, 7465 Trondheim, Norway*
[c] *Danfoss Company, Denmark*
[d] *TLK-Thermo GmbH, 38106 Braunschweig, Germany*
[e] *SINTEF Energy, Kolbjørn Hejes vei 1d, 7465 Trondheim, Norway*

**Abstract**

The continuous derivation of the ambient temperature and cooling demand in $CO_2$ refrigeration and air-conditioning systems equipped with multi-ejector modules for supermarkets requires the analysis of the fixed ejector utilisation in a very wide range of the operational envelope. Therefore, performance mapping of the four R744 ejectors installed in the multi-ejector pack was performed. The investigations of a single ejector's work were performed based on the proposed hybrid reduced-order model to predict the performance of each ejector under arbitrary operating conditions. The proposed model was validated and generated by use of the experimental data together with the computational fluid dynamic model results. The ejector efficiency mapping indicated the area of the best ejector performance in the range from approximately 50 bar to 100 bar. The mass entrainment ratio of all four ejectors was presented for different ambient temperatures and the pressure lift. An area of the mass entrainment ratio greater than 0.3 was obtained by each ejector at ambient temperature above approximately 15 °C for pressure lift below 10 bar. The approximation functions of the ejector pressure lift in terms of the ambient temperature for air-conditioning operating conditions to reach the best efficiency of each ejector are proposed.

*Keywords:* carbon dioxide, refrigeration system, air-conditioning, two-phase ejector, reduced-order model, performance mapping

**Nomenclature**

| | |
|---|---|
| **B** | coefficient matrix, - |
| **C** | covariance matrix, - |
| $h$ | specific enthalpy, J/kg |
| $\dot{m}$ | mass flow rate, kg/s |
| $p$ | pressure, bar |
| $r$ | smoothing factor, - |
| $s$ | specific entropy, J/(kg·K) |
| $t$ | temperature, °C |
| **U** | snapshot matrix, - |
| **V** | modal matrix, - |
| *Greek Symbols* | |
| $\alpha$ | constant coefficient matrix,- |
| *Greek Symbols* | |
| $\chi$ | mass entrainment ratio, - |
| $\delta$ | relative difference, % |
| $\Delta p$ | pressure lift, bar |
| $\Lambda$ | diagonal matrix, - |
| *Subscripts* | |

* Tel.: +48 322372810; fax: +48 322372872
Michal.Haida@polsl.pl



This is the accepted version of an article published in Energy.
DOI: 10.1016/j.energy.2018.04.088

| | | | |
|---|---|---|---|
| $AC$ | air-conditioning | $POD$ | proper orthogonal decomposition |
| $CFD$ | computational fluid dynamics | $RBF$ | radial basis function |
| $EXP$ | experimental data | $ROM$ | reduced order model |
| $MFR$ | mass flow rate | $T$ | transpose matrix |
| $MT$ | medium temperature level | | |

## 1. Introduction

Restrictive regulations regarding refrigerant selection have compelled the use of refrigerants with a negligible impact on global warming and ozone depletion effects [1]. Recently, natural refrigerants, especially carbon dioxide (denoted as R744), have been selected in commercial applications. The satisfactory thermal properties of $CO_2$, as well as its non-flammability, non-toxicity and availability in the market, have led to the use of R744 in supermarket refrigeration applications [2]. Energy performance analyses of the R744 refrigeration system have indicated the necessity to improve the system coefficient of performance (COP) in warm climates due to high thermodynamic losses during system operation in transcritical mode. Therefore, several modifications have been made to improve the system energy performance.

Sharma et al. [3] compared various $CO_2$ supermarket refrigeration system configurations with a typical R410A refrigeration system. The authors stated that the most efficient system was the R744 transcritical booster system with parallel compression in the northern and central parts of the United States of America. This system contained an additional liquid receiver in the intermediate pressure level and an additional compressor to compress the vapour from the receiver into the gas cooler. The liquid phase from the liquid receiver was expanded to the evaporator section. An advanced exergy analysis of the R744 refrigeration booster system with parallel compression was performed by Gullo et al. [4]. The investigation was performed for the ambient temperature of 25°C and 35°C together with the typical cooling demand in the supermarket application. The authors stated that the avoidable exergy destruction of the analysed refrigeration system was mostly endogenous. Moreover, the highest enhancement potential was obtained for the gas cooler/condenser, the high stage compressor and the medium-temperature display cabinet.

Energy performance improvement of the R744 booster system with parallel compression can also be accomplished by using the ejector as the main expansion device to recover some potential work [5]. In a typical supermarket system, the throttling process produces large energy losses due to the irreversible isenthalpic expansion process. An ejector applied to the system can recover some of this energy loss as a result of the entrainment of the low-pressure stream by the high-pressure motive stream under isentropic conditions. Moreover, the entrained stream together with expanded motive stream has higher pressure at the outlet of ejector due to the kinetic energy conversion into the pressure energy. An increase of the pressure reduces the pressure ratio in the compressor section, thereby the electric power consumption decreases and the energy performance of the HVAC&R supermarket system increased. The refrigeration system equipped with an ejector has a higher COP compared to the other system configurations. More information about the R744 ejector-based refrigeration system improvement compared to the conventional system can be found in [6]. Sarkar et al. [7] reported the COP improvement by optimisation of the ejector work in the heat pump system. The similar COP improvement of the R744 refrigeration system equipped with an ejector was obtained by optimisation of the high-side pressure conditions in the work of Xu et al. [8]. In the refrigeration system, the ejector is used either as a vapour ejector or liquid ejector. In the vapour ejector, the R744 vapour stream from the medium-temperature evaporator is compressed without any additional work [9]. The liquid ejector is utilised in the $CO_2$ refrigeration system to pump the liquid outside the medium-temperature evaporator to run the evaporator in flooded mode [10].

$CO_2$ supermarket refrigeration systems operate at different ambient temperatures and different cooling demands, which vary during the daytime. Therefore, the ejector must be designed to work with maximum efficiency at a wide range of these parameters. One strategy for regulating the ejector capacity is to use a controllable ejector [11]. A dynamic simulation of the R744 refrigeration system equipped with a controllable ejector to optimise the multi-variable controller was performed by [12]. The authors stated that the prediction of the optimal gas cooler



This is the accepted version of an article published in Energy.
DOI: 10.1016/j.energy.2018.04.088

pressure improved the energy performance of the system. However, the optimal point of the refrigeration system equipped with the adjustable ejector for best performance was not obtained for the maximum ejector efficiency and cooling capacity [13].

In addition to a controllable ejector, several different fixed-geometry ejectors that can be operated in single mode or parallel mode have been investigated. The multi-ejector concept was presented by Hafner et al. [14], who investigated the energy performance of the R744 multi-ejector supermarket refrigeration system in different European climate zones. The authors showed satisfactory system energy performance improvement of up to 30% compared to the reference $CO_2$ booster system with flash gas bypass and heat recovery. Moreover, Hafner et al. [14] stated that the system control strategy of the multi-ejector system for supermarket application should be optimised to increase the system efficiency in different climate zones.

The R744 multi-ejector expansion pack was designed, manufactured and investigated in the work of Banasiak et al. [15]. The developed module was equipped with four different ejector cartridges to enable a discrete opening characteristic with a binary profile for the R744 vapour compression system. The experimental campaign was performed to map the performance of individual ejectors at the operating conditions typical for a refrigeration system in a supermarket. Moreover, the authors proposed functions for the smallest ejector to calculate the motive nozzle mass flow rate (MFR) and the ratio between the suction nozzle MFR and motive nozzle MFR, called the mass entrainment ratio. The R744 multi-ejector refrigeration system was experimentally investigated by Haida et al. [16]. The experimental analysis indicated improvements of COP and exergy efficiency of up to 8% and 13%, respectively, for the studied system compared to the reference R744 booster system with parallel compression. The authors stated that further improvement of the R744 multi-ejector system could be accomplished by proper design and operation of the refrigeration components for the best integration with the multi-ejector module.

Boccardi et al. [17] analysed a $CO_2$ multi-ejector heat pump system to investigate the effect of different ejector sizes on the global performance and balance of the whole system. The authors stated that the maximum COP can be obtained by system investigation based on optimal multi-ejector module operation to maintain high ejector efficiency of the module. However, the presented multi-ejector was designed for a refrigeration system, which resulted in different performance for the air-conditioning application. Therefore, a multi-ejector module specifically designed for air-conditioning applications should be investigated. Moreover, the optimum ejector performance did not correspond to the system energy performance, and thus a more accurate ejector design is required to improve the R744 multi-ejector system [18].

Integration of the heating, ventilation and air-conditioning systems with the refrigeration system (HVAC&R) in a supermarket application reduced the total electric power consumption of the system by more than 15% [19]. A supermarket system consists of the medium-temperature evaporators and low-temperature evaporators to provide to provide cooling and freezing conditions in the display cabinets, respectively. At the outlet of the evaporators, a working fluid is entered to the liquid receiver and a vapour phase is either compressed in the compressor racks or entrained by the ejector. The high temperature of the discharged refrigerant decreases by the heat rejection in the tap water heating section, space heating section and gas cooler section [20]. Then, the working fluid is expanded either in the electronic expansion valve or inside the ejector, or inside the ejector and partially in the electronic expansion valve. The expanded stream is entered to the separator connected with the air-conditioning evaporator. The vapour phase is directly compressed to the high pressure level in the parallel compressors or expanded in the flash gas bypass valve to the medium-temperature level. The liquid phase from the separator is entered to the evaporation section [20].

A theoretical analysis of the $CO_2$ multi-ejector refrigeration and air-conditioning system was performed by Gullo et al. [21]. The investigated system with a multi-ejector developed by Banasiak et al. [15] was compared with the R404A direct expansion system and various configurations of the R744 booster refrigeration system with and without parallel compression. The theoretical evaluation considered different locations in Southern Europe. The authors stated that the energy savings of the multi-ejector system ranged from 15.6% to 27.3% compared to the R404A direct expansion system. In addition, extrapolation functions of the multi-ejector module mass entrainment ratio were proposed based on the experimental data presented by Haida et al. [16]. The extrapolation functions were limited by the pressure lift, the pressure difference between the suction nozzle and outlet, which varied from 4 bar to 15 bar.

Theoretical investigations of the R744 multi-ejector HVAC&R supermarket system were performed based on the empirical functions of the multi-ejector module provided by experimental results at specified operating con-



This is the accepted version of an article published in Energy.
DOI: 10.1016/j.energy.2018.04.088

ditions. Consequently, the proposed functions can be used only within the specified operating points. The performance of the ejector can be also calculated based on the non-dimensional model developed by Kornhauser et al. [22]. The non-dimensional model was also implemented to the dynamic simulation of the R744 ejector-based refrigeration system by Richter et al. [23]. However, this model assumes the efficiency of the ejector, resulting in low accuracy at the wide ranges found in supermarket applications. Hence, an accurate approximation of the ejector work is required to design an R744 HVAC&R supermarket system equipped with a real ejector. One solution is to perform an experimental investigation. However, the wide range of operating conditions results in a large number of the experimental points. Therefore, a mathematical approach based on a hybrid combination of experimental data with numerical results should be considered for dynamic simulations.

The numerical analysis of the R744 ejector led to the investigation of the local flow phenomena inside the two-phase ejector. These phenomena can be used to either evaluate the performance of the existing ejector or design the ejector under specified operating conditions [24]. Smolka et al. [25] developed a three-dimensional CFD model of the R744 transcritical ejector with a homogeneous equilibrium flow assumption. The authors implemented an enthalpy-based form and real fluid properties from the REFPROP libraries [26] as a substitute for the temperature-based energy equation to simulate carbon dioxide transonic flow inside the two-phase ejector. The accuracy of this homogenous equilibrium model (HEM) was investigated by Palacz et al. [27] for typical supermarket operating conditions. Acceptable accuracy of the HEM results for the R744 two-phase ejector was obtained near or above the critical point. Haida et al. [28] proposed a modified homogeneous relaxation model (HRM), which extended the application range of the CFD model to the subcritical region due to the modification of the relaxation time coefficients. The numerical approach enabled the evaluation of the ejector performance under proper operating conditions, although implementation of each CFD model in dynamic simulations is impossible due to the long computation time for a single operating point.

Calculations of the ejector at high accuracy for refrigeration and air-conditioning operating conditions can be performed by use of the reduced-order model (ROM) based on the proper orthogonal decomposition with radial basis function (POD-RBF). The POD-RBF approach has been used to solve inverse heat transfer problems and in mechanics [29]. This application was also used to build an approximation of the radiative properties of gas mixtures [30]. Moreover, the POD-RBF ROM was used for an R744 two-phase ejector by Haida et al. [31]. An ROM was generated based on the CFD results of the CO2 ejector HEM model for the limited operating conditions close to the critical point. The authors stated that the numerical and experimental validation of the POD-RBF ejector model confirmed the high accuracy of the ROM within ±10% for most of the investigated points. In the present paper , a more advanced approach for an ROM is proposed by combining experimental data and the results of the numerical CFD model of the single ejector to generate the ROM basis for efficient computation of the single operational point. Moreover, the ROM allows functional computation of the R744 ejector within the selected operating points.

The aim of this paper is to present the performance mapping of the fixed ejectors installed in two multi-ejector modules to be integrated with a $CO_2$ HVAC&R supermarket refrigeration system. The hybrid ROM of each ejector was developed based on the experimental data given from an experimental test rig in the SINTEF Energy Research laboratory in Trondheim and the results from an enhanced CFD model of the two-phase ejector performed by using the *ejectorPL* platform [25]. The foregoing platform considers HEM for transcritical conditions [27] and modified HRM two-phase fluid flow assumption for subcritical conditions [28]. Performance mapping was performed to determine the motive nozzle MFR, mass entrainment ratio and ejector efficiency of the investigated ejectors at a wide range of operating conditions. Moreover, the investigation of the pressure lift on ejector performance at the operating conditions typical for supermarket refrigeration, air-conditioning and a heat pump system is presented in this paper.

## 2. The multi-ejector module

Recent R744 supermarket HVAC&R systems are equipped with a multi-ejector module to cover the varying cooling demands in the R744 supermarket refrigeration system. Figure 1 presents the schema of the R744 multi-ejector module with the inlet and outlet ports. The module contained four fixed-geometry ejectors of different sizes. Thus, the capacity of each individual ejector increased in binary order (1:2:4:8). The solenoid valves installed in the motive collector allowed the utilisation of the ejectors in single or parallel operation. The motive



This is the accepted version of an article published in Energy.
DOI: 10.1016/j.energy.2018.04.088

stream entered from the gas cooler outlet, and the suction flow was entrained from the medium-temperature (MT) liquid receiver outside the MT evaporator. The outlet mixed stream flowed to the intermediate-pressure liquid receiver directly connected to the air-conditioning (AC) evaporator. Therefore, the outlet conditions of the multi-ejector were defined based on the AC operational mode. The fixed-geometry ejectors were designed and manufactured in cooperation with SINTEF-SUT-DANFOSS based on the CFD model developed in the work of Smolka et al. [25]. In addition, the multi-ejector model was manufactured, and the performance mapping of each ejector was performed for the refrigeration system operating conditions by Banasiak et al. [15]. The main dimensions of each fixed-geometry ejector are provided in Table 1. During the experimental investigation of the ejectors installed in the multi-ejector module, the efficiency of each ejector for refrigeration operating conditions was of approximately 30% [15]. The similar results of the multi-ejector work was reported by Haida et al. [16]. Moreover, the motive nozzle mass flow rate is clearly dependent on the inlet density and the inlet pressure, thereby the pulsation flow of the motive nozzle stream in each ejector was reduced by the proper designing and manufacturing processes [15].

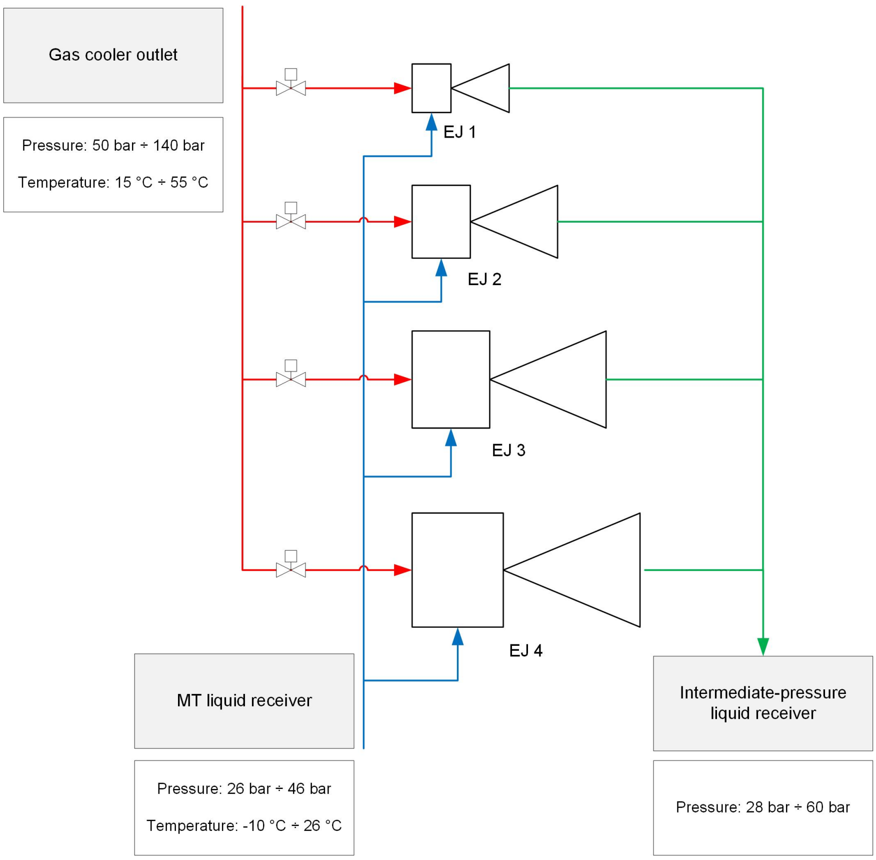


Figure 1: The R744 multi-ejector module with four vapour ejectors.

The performance mapping of the fixed-geometry ejectors installed in the multi-ejector module was performed at a much wider operating regime than that used by Banasiak et al. [15] to investigate the ejector efficiency of the ejector in a $CO_2$ HVAC&R supermarket system. The operational envelope for the motive nozzle and the suction nozzle of the ejectors is presented in Figure 2. The same operating regimes was defined for all four vapour ejectors installed in the multi-ejector module to map the performance of each individual ejector at the same HVAC&R supermarket operating conditions. As shown in Figure 2(a) the motive nozzle pressure was defined in the range from 50 bar to 140 bar to analyse the ejector performance in subcritical and transcritical operating modes at various ambient temperatures. In addition, the motive nozzle temperature was defined in the range from 5 °C to 55 °C. The suction nozzle operating conditions presented in Figure 2(b) were defined to analyse the ejector map-



This is the accepted version of an article published in Energy.
DOI: 10.1016/j.energy.2018.04.088

Table 1: The main geometry parameters of the fixed-geometry ejectors installed in the R744 multi-ejector module [15].

| Parameter name | Unit | EJ 1 | EJ 2 | EJ 3 | EJ 4 |
|---|---|---|---|---|---|
| Motive nozzle inlet diameter | $10^{-3}$ m | 3.80 | 3.80 | 3.80 | 3.80 |
| Motive nozzle throat diameter | $10^{-3}$ m | 1.00 | 1.41 | 2.00 | 2.83 |
| Motive nozzle outlet diameter | $10^{-3}$ m | 1.12 | 1.58 | 2.24 | 3.16 |
| Motive nozzle converging angle | $^\circ$ | 30.00 | 30.00 | 30.00 | 30.00 |
| Motive nozzle diverging angle | $^\circ$ | 2.00 | 2.00 | 2.00 | 2.00 |
| Diffuser outlet diameter | $10^{-3}$ m | 7.30 | 8.40 | 10.30 | 13.10 |
| Diffuser angle | $^\circ$ | 5.00 | 5.00 | 5.00 | 5.00 |

ping performance for superheated vapour with superheat below 15 K, saturated vapour and two-phase flow with quality above 0.8. Moreover, the suction nozzle pressure varied in the range from 26 bar to 46 bar related to the refrigeration, AC and heat pump conditions. The outlet conditions were defined by the difference between the outlet pressure and suction nozzle pressure, which is called the pressure lift $\Delta$p. In the presented investigation, the pressure lift for all ejectors was in the range from 4 bar to 15 bar. The outlet conditions were presented in Figure 2(c). The set of the operating conditions is presented in Table 2.

Table 2: The operating conditions of all four ejectors installed in the multi-ejector module.

| Boundary condition | Motive nozzle | | Suction nozzle | | | | Outlet |
|---|---|---|---|---|---|---|---|
| Parameter | Pressure | Temperature | Pressure | Quality | Temperature | Superheat | Pressure |
| Unit | bar | $^\circ$C | bar | - | $^\circ$C | K | bar |
| Min | 50 | 5 | 26 | 0.8 | -10.65 | 0 | 28 |
| Max | 140 | 55 | 46 | 1.0 | 25.87 | 15 | 60 |

The wide operating range required the use of a complex mathematical model to predict the two nozzles' MFRs for each ejector. However, the mathematical model must also be adapted to perform the ejector calculation in a dynamic simulation of a $CO_2$ HVAC&R supermarket system with respect to the energy performance analysis of the system. Therefore, the proposed hybrid ROM was used in the presented investigation because the main benefits of ROM are fast computations and high accuracy of the mass flow rate prediction.

## 3. Hybrid ROM

The hybrid ROM was developed based on the proper orthogonal decomposition with the radial basis function interpolation approach. The most important advantage of such a choice for the approximation base is its optimality. Moreover, the RBF interpolation method allows the ROM to be a continuous function of the arbitrary input parameters [32]. The hybrid ROM is an enhanced model of the developed POD-RBF ROM that was based only on the CFD results presented in [31]. The CFD-based ROM of the $CO_2$ ejector was investigated and the global and local parameters of the two-phase flow inside the ejector given by ROM were compared with the numerical results as well as the experimental data. In this paper, the POD-RBF model was generated based on the CFD results and the experimental data to ensure high accuracy of the ROM results within the wide operating regime. The mathematical approach for the ROM is presented in Section 3.1 and the validation of the hybrid ROM is described in Section 3.2.



This is the accepted version of an article published in Energy.
DOI: 10.1016/j.energy.2018.04.088

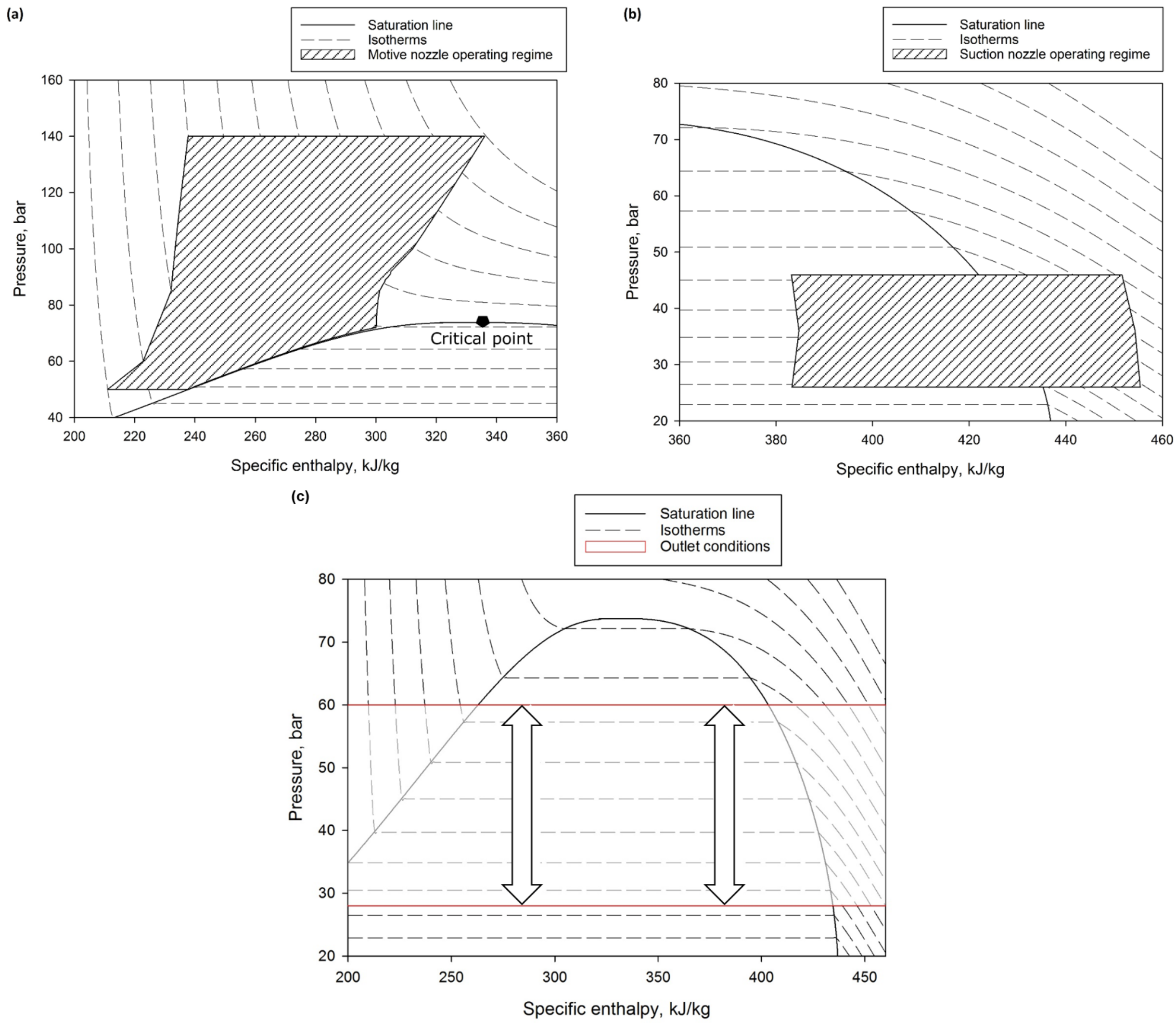


Figure 2: The operational envelope on a pressure-specific enthalpy diagram of each R744 vapour ejector installed in the multi-ejector module: (a) motive nozzle; (b) suction nozzle; (c) outlet.



This is the accepted version of an article published in Energy.
DOI: 10.1016/j.energy.2018.04.088

### 3.1. POD-RBF approach

The POD approach constructs the optimal approximation base based on the set of $N$ sampled values of the two-phase flow parameters inside the ejector stored in a single vector called the snapshot [32]. Thus, the snapshot rectangular matrix $\mathbf{U}$ is generated for $M$ snapshot vectors related to the number of the considered operating points (which are the input parameters used to generate the snapshots). The snapshot vectors are thus related to the input parameters. The aim of POD is to find the orthogonal matrix $\Phi$ by reconstructing the snapshot matrix $\mathbf{U}$ based on the linear combination of the snapshots:

$$\Phi = \mathbf{U} \cdot \mathbf{V} \tag{1}$$

where $\mathbf{V}$ is the modal matrix defined in the following eigenvalue problem as a nontrivial solution:

$$\mathbf{C} \cdot \mathbf{V} = \Lambda \cdot \mathbf{V} \tag{2}$$

where $\Lambda$ is the diagonal matrix and $\mathbf{C}$ is the positive covariance matrix defined as follows:

$$\mathbf{C} = \mathbf{U}^T \cdot \mathbf{U} \tag{3}$$

where $\mathbf{U}^T$ is a transposed snapshots matrix. In this situation, when the covariance matrix is known, the POD basis can be computed directly by solving an eigenvalue problem:

$$\mathbf{C} \cdot \phi^i = \lambda_i \cdot \phi^i \tag{4}$$

where $\phi^i$ is the orthogonal POD basis vector and $\lambda_i$ are the eigenvalues stored by the diagonal matrix $\Lambda$. In the Karhunen-Loève transformation technique, the real and positive eigenvalues should be sorted in descending order. The snapshots are strongly correlated with each other when the eigenvalues decrease rapidly along with increasing mode number. Therefore, the POD model can use only part of the POD modes to obtain a high accuracy approximation. The truncated POD model $\bar{\Phi}$ considers $K < N$ elements for $M$ operating points, which decreases the orthogonal matrix $\bar{\Phi}$ size.

$$\bar{\Phi} = \mathbf{U} \cdot \bar{\mathbf{V}} \tag{5}$$

where $\bar{\mathbf{V}}$ is the truncated modal matrix with first $K$ eigenvectors of covariance matrix $\mathbf{C}$. The truncated POD basis is orthogonal and achieves optimal approximation properties. The snapshot reconstruction based on the truncated approximation formula must be performed depending on the additional parameters used in the snapshot generation. Hence, an arbitrary snapshot can be defined as follows:

$$\mathbf{u}^j \approx \sum_{k=1}^{K} \bar{\Phi}^k \alpha_k^j \tag{6}$$

where $\mathbf{u}^j$ is the vector of the arbitrary snapshot, $\bar{\Phi}^k$ is the $k$-element of the truncated orthogonal basis and $\alpha_k^j$ is the unknown coefficient vector related to the parameters used to create the snapshots. The foregoing approximation is valid only for the snapshots used to build the POD basis. When the two-phase ejector is utilised in a wide range of motive nozzle, suction nozzle and outlet operating conditions, the POD model requires an additional interpolation procedure to evaluate the ejector behaviour outside the operating points chosen in the course of POD basis construction. Based on the arbitrary snapshot equation presented in Eq. (6), the snapshot matrix $\mathbf{U}$ can be defined as a linear combination of the truncated POD vectors:

$$\mathbf{U} = \bar{\Phi} \cdot \bar{\alpha} \tag{7}$$

where $\bar{\alpha}$ is the unknown constant coefficients matrix, which can be computed as the transpose matrix of the orthogonal truncated POD basis $\Phi^T$ multiplied by the snapshot matrix:

$$\bar{\alpha} = \bar{\Phi}^T \cdot \mathbf{U} \tag{8}$$



This is the accepted version of an article published in Energy.
DOI: 10.1016/j.energy.2018.04.088

In proposed ROM, the unknown coefficients matrix $\bar{\alpha}$ was defined as a non-linear function of the input parameters. Therefore, the foregoing coefficients matrix can be defined as follows:

$$\bar{\alpha} = \mathbf{B} \cdot \mathbf{F} \tag{9}$$

where **B** is the matrix of the unknown coefficients of the selected combination and **F** is the matrix of the interpolation functions $f_i\left(k - k^i\right)$ for the set of $k$ parameters identical to the values used to build the subsequent snapshots. The radial basis interpolation functions were applied for the presented ROM because the RBF interpolation is mostly used for multidimensional approximation. In this study, the thin plate spline radial function with a smoothness factor was employed:

$$f_i\left(|k - k^i|\right) = \left(\frac{|k - k^i|}{r}\right)^2 \cdot \ln\left(\frac{|k - k^i|}{r}\right) \tag{10}$$

where $|k - k^i|$ is the distance between the current set of the parameters $k$ and the reference set of the parameters $k^i$, $r$ is the smoothing factor. Considering the foregoing definition of the $i^{th}$ interpolation function, the matrix **F** takes the following form:

$$\mathbf{F} = \begin{bmatrix} f_1\left(|k^1 - k^1|\right) & \cdots & f_1\left(|k^j - k^1|\right) & \cdots & f_1\left(|k^M - k^1|\right) \\ \vdots & & \vdots & & \vdots \\ f_i\left(|k^1 - k^j|\right) & \cdots & f_i\left(|k^j - k^j|\right) & \cdots & f_i\left(|k^M - k^j|\right) \\ \vdots & & \vdots & & \vdots \\ f_M\left(|k^1 - k^M|\right) & \cdots & f_M\left(|k^j - k^M|\right) & \cdots & f_M\left(|k^M - k^M|\right) \end{bmatrix} \tag{11}$$

After the generation of the **F** matrix, the matrix **B** defined in Eq. (9) can be computed by use of the singular value decomposition technique [33]. Finally, snapshot generation by use of the arbitrary parameter set $k$ can be defined by the following equation:

$$\mathbf{u}^a(k) \approx \bar{\Phi}\mathbf{B}\mathbf{f}^a(k) \tag{12}$$

where $\mathbf{u}^a(k)$ is the calculated snapshot based on the arbitrary parameter set $k$ and $\mathbf{f}^a(k)$ stands for vector of interpolation functions defined in Eq. (10). The implementation of RBF into the POD model reduces the dimensionality of ROM to the number of unknown parameters $k$. The unknown parameters are defined as the boundary conditions of the $CO_2$ two-phase ejector as follows:

- Motive nozzle pressure
- Motive nozzle specific enthalpy
- Suction nozzle pressure
- Suction nozzle specific enthalpy
- Outlet pressure

The specific enthalpy for the motive nozzle and the suction nozzle was defined to perform the calculations either for one-phase conditions or two-phase conditions. The snapshot generated from the CFD results was prepared in a similar manner as the snapshot based on the experimental data to use both inputs in the hybrid ROM basis. The single snapshot was defined as the set of motive nozzle and suction nozzle MFRs for a single boundary condition.

The CFD model of the R744 two-phase ejector was developed by Smolka et al. [25]. The enthalpy-based energy equation formulation was implemented to obtain real fluid properties of $CO_2$ flow in the two-phase region. The fluid properties of the R744 two-phase flow were obtained from REFPROP libraries [26]. The CFD model calculations were performed based on two fluid flow assumption models: the homogeneous equilibrium model (HEM) and modified homogeneous relaxation model (HRM). HEM was used to predict MFRs in the supercritical region



This is the accepted version of an article published in Energy.
DOI: 10.1016/j.energy.2018.04.088

and close to the critical point for which the HEM application range was defined [27]. The modified HRM provides motive nozzle and suction nozzle MFR accuracy within ±10% for the subcritical operating regime due to the optimisation of the relaxation time correlation [28].

The realisable $k-\epsilon$ turbulence model in HEM approach and the $k-\omega$ SST model in the modified HRM approach to model the R744 two-phase turbulent flow inside the ejector [34]. The realisable $k-\epsilon$ turbulence model applied in the HEM for CO2 two-phase ejector was tested by Smolka et al. [25] with successful results. Moreover, this turbulence model was also used to define application range of HEM for R744 two-phase ejector in the work of Palacz et al. [27]. According to Mazzelli et al. [35], the $k-\omega$ SST model showed the best agreement of the global and local flow parameters inside the ejector. During the numerical investigation of the modified HRM, the $k-\omega$ SST model properly predicted the mixing process of both streams inside the pre-mixer and the mixing chamber. More information about the turbulence model can be found in [28].

The CFD model with both fluid flow assumptions was validated, and the numerical mesh grid was investigated. In the work of Smolka et al. [25], a three-dimensional numerical model of a $CO_2$ two-phase ejector was investigated. Moreover, the mesh sensitivity analysis of the three-dimensional and two-dimensional axisymmetric model of the two-phase ejectors installed in the multi-ejector module was done by Palacz et al. [36]. According to the ejectors shape, the numerical model of each ejector was defined as the two-dimensional axisymmetric CFD model, which significantly reduced the size of the numerical grid. Hence, the mesh was generated by approximately 20,000 hexahedral elements. Moreover, the minimum orthogonal quality was 0.9, confirming the negligible influence of element shape on the results. The wall roughness was set to 2 $\mu$m according to the ejectors manufacturers [37]. The partial differential equations of the mathematical model were solved based on the PRESTO scheme for the pressure discretisation and the second-order upwind scheme for the other variables considered in the CFD model. Moreover, the coupled method was employed for the coupling of the velocity and pressure fields.

The automation of the geometry and mesh preparation together with the CFD calculation and the post-processing was performed by developing the *ejectorPL* platform. This platform has been successfully used in several numerical investigations of the $CO_2$ ejector, i.e. parametrisation procedure of the R744 liquid ejectors [10], swirling of the motive and suction streams for ejector performance improvement [38], shape optimisation of the R744 two-phase ejector [39] and numerical investigation of the multi-ejector module during single and parallel operation [40]. Therefore, the CFD results used to generate the hybrid ROM basis were obtained by use of the *ejectorPL* platform. More detailed information about the numerical approach used for the mapping performance can be found in [25]. Moreover, the description about HEM approach together with the application range was presented by Palacz et al. [27]. An information about the modified HRM used to generate hybrid ROM together with the experimental data as well as the application range can be found in [28].

The validation procedure of the CFD model was accomplished based on the experimental data of the fixed-geometry ejectors installed in the multi-ejector module. The test campaign was conducted on the R744 multi-ejector vapour compression test rig in the SINTEF laboratory in Trondheim, Norway. The multi-ejector module was utilised either in single operation for each vapour ejector or in parallel operation. The test facility was fully equipped with pressure, temperature and mass flow rate sensors, and the accuracies of these sensors were taken from the relevant product data sheets. The temperature was measured by a PT1000 resistance thermometer with an accuracy of $\pm(0.3 + 0.005\ t)$, where $t$ is the temperature in °C. A piezoelectric transmitter was used to measure the pressure with an accuracy of ±0.3% of reading. The mass flow rate was measured by using Coriolis type RHM06 and RHM15 transducers, and the accuracy was ±0.2% of the reading. The output signals from the sensors installed in the test rig were processed and transmitted by the Danfoss control unit to the Danfoss Minilog system. More details about the test facility can be found in the work of Haida et al. [16].

The use of the experimental data together with the high-accuracy CFD results to generate the hybrid ROM of each $CO_2$ ejector permitted the evaluation of the ejector performance under the refrigeration, air-conditioning and heat-pump operating conditions in the supermarket system. The ejector work can be presented by use of the mass entrainment ratio and ejector efficiency definitions. The mass entrainment ratio is the ratio between the suction nozzle MFR and the motive nozzle MFR:

$$\chi = \frac{\dot{m}_{SN}}{\dot{m}_{MN}} \tag{13}$$

where $\chi$ is the mass entrainment ratio and $\dot{m}$ is the mass flow rate in kg/s of the motive nozzle (MN) and the



This is the accepted version of an article published in Energy.
DOI: 10.1016/j.energy.2018.04.088

suction nozzle (SN). The ejector efficiency was defined by Elbel et al. [9] as the ratio of the amount of the recovered ejector expansion work rate with maximum possible expansion work rate recovery potential:

$$\eta_{ej} = \frac{\dot{W}_{rec}}{\dot{W}_{rec,max}} = \chi \cdot \frac{h(p_{out}, s_{SN}) - h(p_{SN}, s_{SN})}{h(p_{out}, s_{MN}) - h(p_{MN}, s_{MN})} \tag{14}$$

where $\eta_{ej}$ is the ejector efficiency, $\dot{W}$ is the expansion work rate in W, $h$ is the specific enthalpy in J/kg, $p$ is the pressure in Pa and $s$ is the specific entropy in J/(kg·K). In this paper, the ejector efficiency and the mass entrainment ratio were presented for each investigated ejector to indicate the area of best ejector performance under different operating conditions. Hence, the hybrid ROM of the ejectors installed in the multi-ejector module was validated with the experimental data to ensure high accuracy of the MFR prediction. The MFR discrepancy of the hybrid ROM was calculated as the relative error between the experimental data and the hybrid ROM result:

$$\delta_{MFR} = 1 - \frac{\dot{m}_{hybridROM}}{\dot{m}_{exp}} \cdot 100\% \tag{15}$$

where $\delta_{MFR}$ is the relative error of the motive nozzle MFR or the suction nozzle MFR obtained by the hybrid ROM.

### 3.2. Hybrid ROM validation

The hybrid ROM was validated for all the investigated ejectors using three different sets of input data: the CFD results without the experimental data, the CFD results with 50% (selected randomly) of the experimental data for the entire operating regime, and the CFD results with all experimental data. Randomly selected 50% results of the experimental data were chosen from different motive nozzle conditions (subcritical, transcritical, close to the critical point) and suction pressure together with the different pressure lift. The integration of the experimental data with the CFD results in the POD basis permitted the prediction of the MFR of both nozzles either in the CFD operating points or in the experimental operating points or between them. Figure 3 presents the hybrid ROM motive nozzle MFR accuracy of the fixed-geometry ejector EJ 2 from Table 1. The results are shown on the pressure-specific diagram together with the pressure lift to evaluate the model accuracy at different motive nozzle conditions and the difference between the outlet pressure and the suction nozzle pressure. Moreover, the different sets of input data were taken into account in the validation procedure. The prediction of the motive nozzle MFR of a hybrid ROM with different input data let to define an influence of the selected experimental data to generate hybrid ROM on the accuracy of the motive nozzle MFR. As shown in Figure 3(a), the ROM based only on the CFD results obtained satisfactory high accuracy for the motive nozzle pressure above 70 bar. The motive nozzle MFR discrepancy below ±5% was obtained for transcritical conditions in the motive nozzle and all points for pressure lift above 8 bar. The decrease of the pressure lift for motive nozzle pressure above 70 bar slightly decreased the accuracy. Hence, the MFR prediction was within ±10% for some operating points at pressure lift below 8 bar, especially for pressure lift of approximately 3 bar. A motive nozzle MFR discrepancy above ±10% was obtained below 60 bar in the CFD model MFR prediction. The integration of the CFD results with 50% of the experimental data presented in Figure 3(b) revealed a much higher motive nozzle MFR accuracy of the hybrid ROM compared to the ROM based only on the CFD results. Moreover, satisfactory accuracy within ±10% was obtained in the entire operating regime, with only several operating points above ±10%. It can be seen that the integration of the 50% of the experimental data strongly influenced on the MFR prediction in the subcritical region for the motive nozzle pressure below 60 bar, where the CFD model obtained higher discrepancy when compared to the operating conditions above 60 bar. Hence, the hybrid ROM let to predict motive nozzle MFR at high accuracy within ±5% for refrigeration, air-conditioning and heat-pump applications. The hybrid ROM based on the CFD results and all the experimental data achieved a motive nozzle mass flow rate accuracy within ±5% at all operating conditions. It can be seen that the hybrid ROM accuracy strongly related on the CFD model accuracy and the MFRs prediction of the hybrid ROM can be improved by add of the experimental data in the throughout operating regime. Therefore, the integration of the CFD results with the experimental data in the hybrid ROM of the $CO_2$ ejector let to predict the performance of the ejector with highly satisfactory accuracy.

Table 3 presents the set of hybrid ROM validation procedure results as the MFR discrepancy range of each hybrid ROM for all considered experimental points. Based on the validation presented in Figure 3 for EJ 2, the



This is the accepted version of an article published in Energy.
DOI: 10.1016/j.energy.2018.04.088

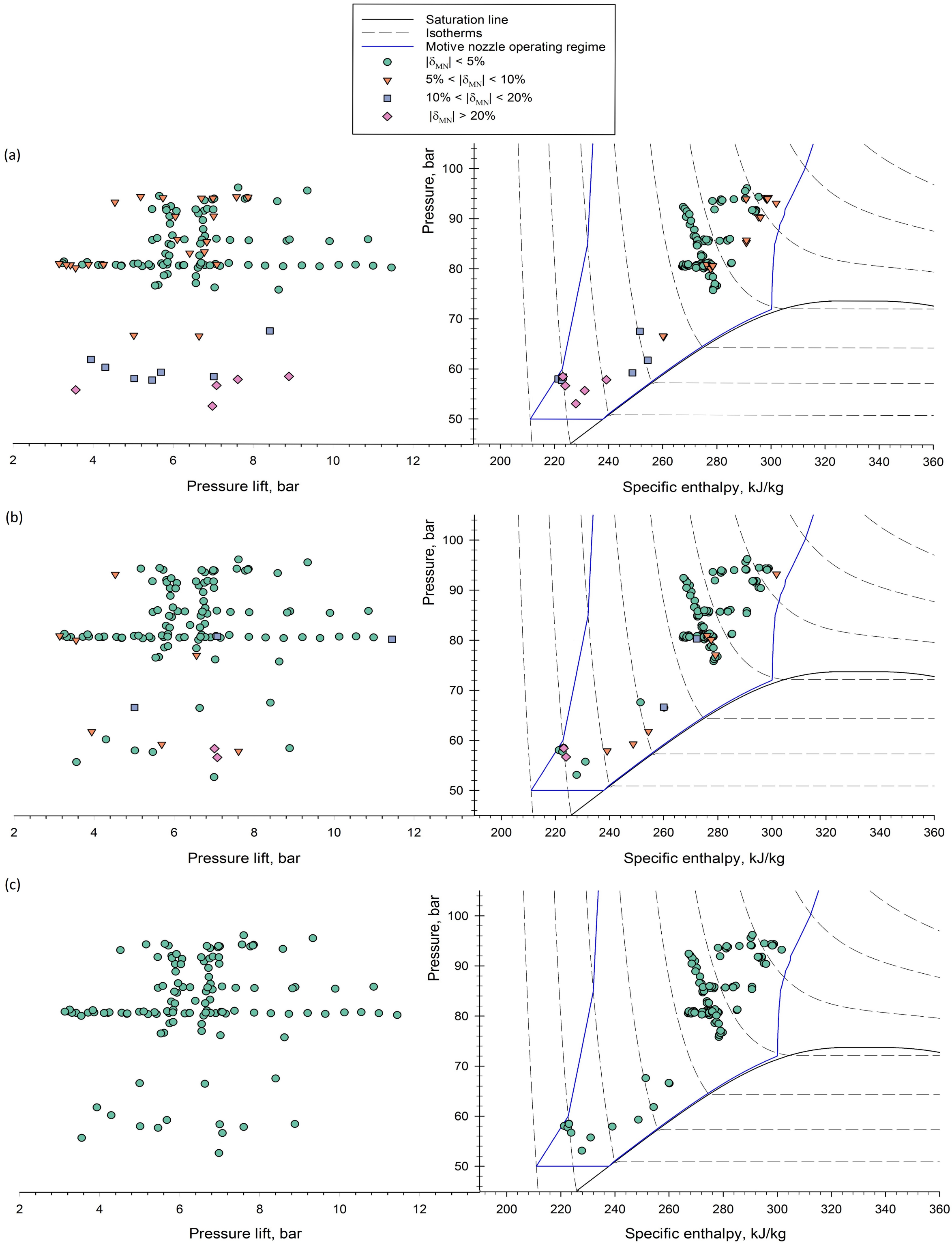


Figure 3: The hybrid ROM motive nozzle MFR discrepancy of the fixed-geometry ejector EJ 2 from Table 1 with different input data: (a) only CFD results; (b) CFD results and 50% of the experimental data; (c) CFD results and 100% of the experimental data.



This is the accepted version of an article published in Energy.
DOI: 10.1016/j.energy.2018.04.088

Table 3: The set of the hybrid ROM motive nozzle and the suction nozzle MFR accuracies for all experimental points considered in the validation.

| Input data | EJ 1 | | EJ 2 | | EJ 3 | | EJ 4 | |
|---|---|---|---|---|---|---|---|---|
| | $\lvert\delta_{MN}\rvert$ | $\lvert\delta_{SN}\rvert$ | $\lvert\delta_{MN}\rvert$ | $\lvert\delta_{SN}\rvert$ | $\lvert\delta_{MN}\rvert$ | $\lvert\delta_{SN}\rvert$ | $\lvert\delta_{MN}\rvert$ | $\lvert\delta_{SN}\rvert$ |
| CFD + 50% experimental data | <5% | <10% | <5% | <10% | <5% | <15% | <5% | <15% |
| CFD + 100% experimental data | <1% | <1% | <1% | <1% | <1% | <1% | <1% | <1% |

hybrid ROM used two different input data: the CFD results with 50% (selected randomly) of the experimental data for the entire operating regime, and the CFD results with all experimental data. Moreover, the prediction of the motive nozzle and suction nozzle MFRs was validated in the entire operating regime presented in Figure 2 and the average accuracy range was presented. The motive nozzle MFR accuracy of each ejector was within ±5% for the hybrid ROM based on the CFD results together with 50% of all experimental data. The high accuracy of the motive nozzle MFR prediction by the hybrid ROM based on the CFD results together with 50% of all experimental data confirmed that the integration of the experimental data together with CFD results let to perform the calculation of the ejector at different cooling capacity and operating conditions for HVAC&R supermarket system. This hybrid ROM obtained a suction nozzle MFR discrepancy within ±10% for EJ1 and EJ2. For the larger ejectors, EJ3 and EJ4, a suction nozzle MFR within ±15% was predicted by the hybrid ROM based on the CFD results together with 50% of all experimental data. An increase of the number of the experimental data considered in the input data of hybrid ROM improved the accuracy of the both nozzles MFR. The use of all experimental data with the CFD results to generate the hybrid ROM allowed the prediction of the MFR of both nozzles with an accuracy within ±1% at every validated operating point. The very high accuracy of the hybrid ROM based on the CFD results and all experimental data let to implement the hybrid ROM into the R744 supermarket system simulations to evaluate the energy performance of the ejector-based system at different operating conditions and cooling demand. Hence, the performance mapping of each investigated ejector was performed for different application operating conditions that can be found in a supermarket HVAC&R system. Moreover, increasing the experimental data considered in the trained POD basis resulted in hybrid ROM improvement.

## 4. The R744 ejectors performance mapping

The validation procedure confirmed that the hybrid ROM of the $CO_2$ ejectors installed in the multi-ejector module predicted the motive nozzle and suction nozzle MFRs with satisfactory accuracy within the operating envelope. Hence, performance mapping of the investigated ejectors was performed to define the ejector work recovery potential at different operating conditions. The investigation was performed under a typical operating regime for refrigeration system, air-conditioning system and heat pump applications. The ejector mapping was performed for the global ejectors parameters: motive nozzle MFR, the ejector efficiency, mass entrainment ratio and pressure lift to indicate the maximum potential of the ejectors to cover the cooling demand and the area of the best performance. The local parameters of the investigated ejectors i.e. velocity or absolute pressure fields were presented by Haida et al. [31], where ROM was developed based on the CFD results given by *ejectorPL* platform and the comparison of different snapshots size together with the CFD results and experimental data was shown. The local phenomena, i.e. Mach number, pressure distribution etc. were presented during the numerical investigation of the foregoing ejectors, especially for the optimisation procedure of the mixer shape and ejector shape [36, 39]. In this paper, the mapping performance of all ejectors was done to define the work of each ejector at the operating conditions defined by pressure, specific enthalpy and temperature. Hence, the relationship between the other $CO_2$ flow parameters i.e. density or entropy is related to the HVAC&R supermarket system operating conditions. The hybrid ROM were implemented in Microsoft Excel software as a dynamic link-library (DLL) to perform fast calculations of the ejector MFRs at the specified operating conditions. The fluid properties of $CO_2$ were taken from REFPROP libraries [26].



This is the accepted version of an article published in Energy.
DOI: 10.1016/j.energy.2018.04.088

The motive nozzle MFR mapping of the R744 vapour ejectors is presented in Figure 4. The investigation was performed for all four fixed-geometry ejectors within the operating regime of the motive nozzle. The suction nozzle pressure was set to approximately 26 bar with a superheat of 5 K and pressure lift of 4 bar. The operating conditions of the suction nozzle and the outlet were set typical for refrigeration application regarding the MT evaporation temperature of -10 °C [21]. Each ejector obtained the lowest value of the motive nozzle MFR close to the saturation line, but the highest values indicated a pressure of 140 bar and specific enthalpy of approximately 220 kJ/kg. Figure 4(a) shows that the motive nozzle MFR of EJ 1 varied in the range from 0.1 kg/s to less than 0.01 kg/s. The constant MFR lines were set almost parallel to the saturation line. Therefore, an increase in the gas cooler subcooling in the subcritical region resulted in an increase in the motive nozzle MFR. In the transcritical and supercritical regime, EJ 1 reached higher values of the motive nozzle MFR during the decrease in the temperature at constant pressure. Hence, the proper selection of the gas cooler outlet temperature influenced the ejector capacity. A similar trend was obtained for ejector EJ 2 in Figure 4(b). However, the motive nozzle MFR varied in the range from approximately 0.03 kg/s to 0.17 kg/s, approximately two times larger than the range for EJ 1. Hence, the capacity of EJ 2 was able to cover a twofold higher cooling demand of the refrigeration system compared to EJ 1. For EJ 3, as presented in Figure 4(c), the motive nozzle MFR mapping was similar to that of EJ 2, and the values of MFR were in the range from approximately 0.1 kg/s to 0.34 kg/s. The lowest value of the motive nozzle MFR was indicated for the pressure in the range from 50 bar to 60 bar and close to the saturation line. Slightly different trends of the motive nozzle MFR were observed for the largest ejector, EJ 4, compared with the other investigated ejectors, as shown in Figure 4(d). The increase in the motive nozzle MFR at constant specific enthalpy was much lower in the pressure range from 80 bar to 110 bar. Hence, the capacity of EJ 4 within that region was slightly different, and further increases in the pressure resulted in a greater increase in the motive nozzle MFR. The utilisation of all ejectors either in single operating mode or in parallel mode covered the wide range of the cooling demand for the supermarket application. Moreover, the proper selection of the gas cooler outlet conditions affected the multi-ejector capacity, which influenced the selection of the running ejectors. The similar map of the each ejector motive nozzle MFR confirmed that the capacity of the multi-ejector module can be covered by individual work of the selected ejector or by parallel work of the ejectors in different combinations. However, the information about the ejector efficiency let to evaluate the best combination of the multi-ejector work for best system performance.

Figure 5 presents the ejector efficiency mapping of the fixed-geometry ejectors installed in the multi-ejector module. The hybrid ROM ejector efficiency results are presented within the specified motive nozzle operating regime. The suction nozzle pressure was approximately 26 bar at an MT evaporation temperature of -10 °C with a superheat of 5 K and a pressure lift of 4 bar for each investigated ejector. The ejector efficiency of all four $CO_2$ ejectors was below 0.4. As shown in Figure 5(a), the ejector EJ 1 exhibited the best performance for the motive nozzle pressure in the range from 60 bar to 80 bar. Moreover, an ejector efficiency above 0.2 was reached in the subcritical region as well as in the transcritical region. The low value of the ejector efficiency was observed at motive nozzle pressures above 120 bar. Similar ejector performance mapping was obtained for EJ 2, as shown in Figure 5(b). An ejector efficiency above 0.2 was observed for the motive nozzle pressure in the range from 50 bar to 120 bar. Moreover, the highest efficiency of EJ 2 was obtained at a specific enthalpy below 240 kJ/kg and a pressure of approximately 70 bar. EJ 3 exhibited an ejector efficiency above 0.2 for most of the investigated points for the motive nozzle pressure from 50 bar to 120 bar, as shown in Figure 5(c).However, the efficiency of EJ 3 was lower than 0.2 for the motive pressure above 120 bar and close to the saturation line in the subcritical region. The ejector efficiency mapping of EJ 4 presented in Figure 5(d) was slightly different when compared with the other ejectors as the result of the ejector capacity and the motive nozzle MFR. The highest ejector efficiency was obtained for the wider motive nozzle operating regime for the pressure in the range from 60 bar to 100 bar. Moreover, the efficiency of EJ 4 above 0.2 was within the same range as for the smaller ejectors, and the lowest efficiency was obtained above approximately 120 bar and close to the saturation line in the subcritical region. Therefore, each investigated ejector installed in the multi-ejector module obtained high efficiency to recover some potential work and improve the COP of the refrigeration system. Moreover, the energy performance improvement of the system was strongly related to the ejector performance as well as the operating conditions of the gas cooler and MT or AC evaporators. The high efficiency of the multi-ejector module for different cooling demand can be obtained by selection of the running ejectors that maintained high efficiency at defined operating conditions in the $CO_2$ supermarket system.

The R744 refrigeration system equipped with the multi-ejector module exhibited improved energy perfor-



This is the accepted version of an article published in Energy.
DOI: 10.1016/j.energy.2018.04.088

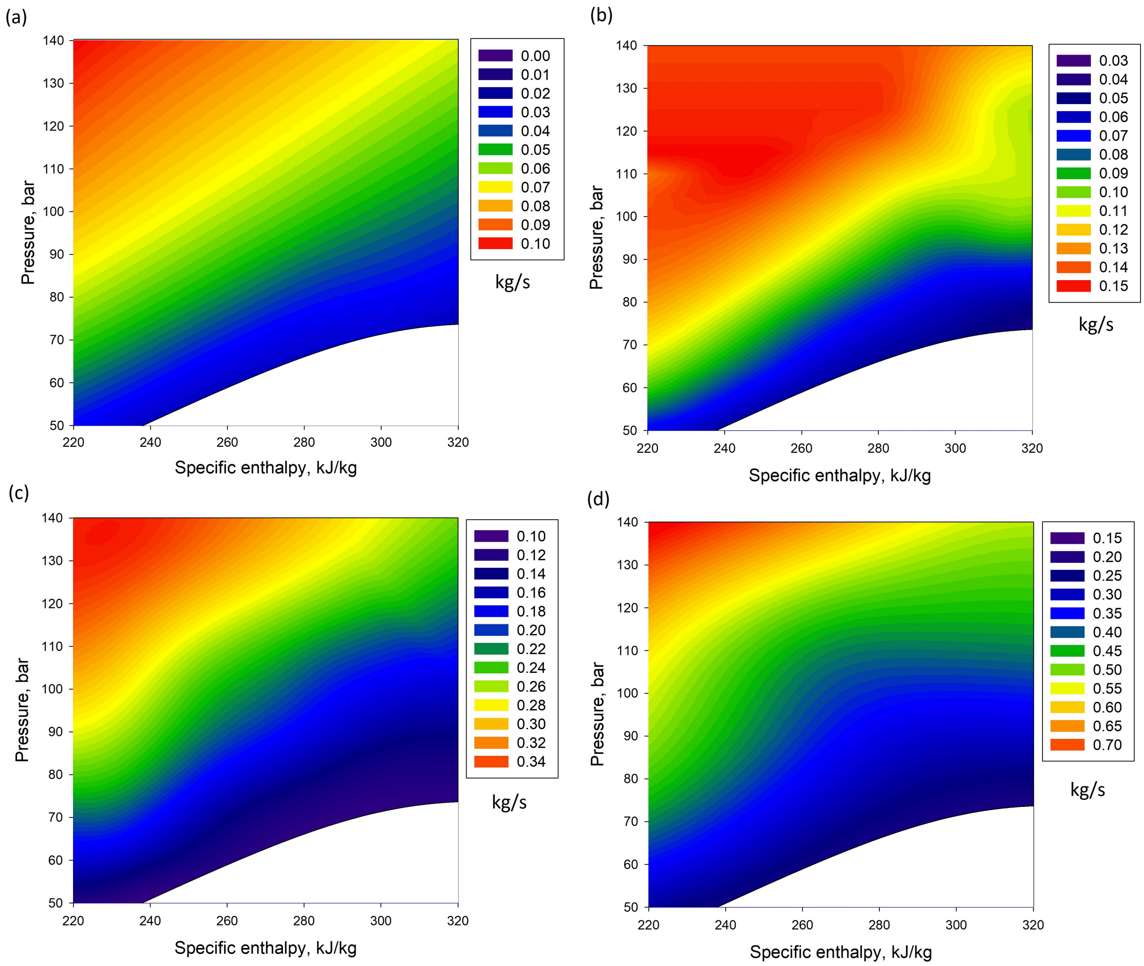


Figure 4: The motive nozzle MFR mapping of the investigated R744 ejectors at the MT evaporation temperature of -10 °C with the superheat of 5 K and the pressure lift of 4 bar: (a) EJ 1; (b) EJ 2; (c) EJ 3; (d) EJ 4.

mance compared with the standard R744 booster system with parallel compression in both the experimental investigation [16] and the theoretical investigation for different localisations of the supermarket system [21]. However, the analysis indicated the possibility of improving the system energy performance by optimising the pressure lift in the multi-ejector module. Hence, information about the mass entrainment ratio and the pressure lift of the fixed-geometry ejectors at different ambient temperatures was obtained to define the application area of the investigated ejectors in the supermarket HVAC&R system.

Figure 7 presents the investigation of the mass entrainment ratio of the four R744 fixed-geometry ejectors installed in the multi-ejector module. The motive nozzle conditions presented in Figure 6 were defined in terms of the ambient temperature to obtain the best performance of the gas cooler based on the correlation presented by Gullo et al. [21]. The ambient temperature was in the range from 5 °C to 50 °C to analyse the ejector performance for the refrigeration application as well as the heat pump application [18]. The suction nozzle conditions were set based on the MT evaporation temperature of -4 °C for the flooded MT evaporator [21]. Each ejector exhibited similar trends of $\chi$ in terms of the different pressure lifts. The first ejector EJ 1 presented in Figure 7(a) obtained $\chi$ above 0.3 for the ambient temperature in the range from 15 °C to 45 °C at different pressure lift. Moreover, EJ 1 reached $\chi$ of approximately 0.3 for pressure lift of approximately 10 bar and the ambient temperature of



This is the accepted version of an article published in Energy.
DOI: 10.1016/j.energy.2018.04.088

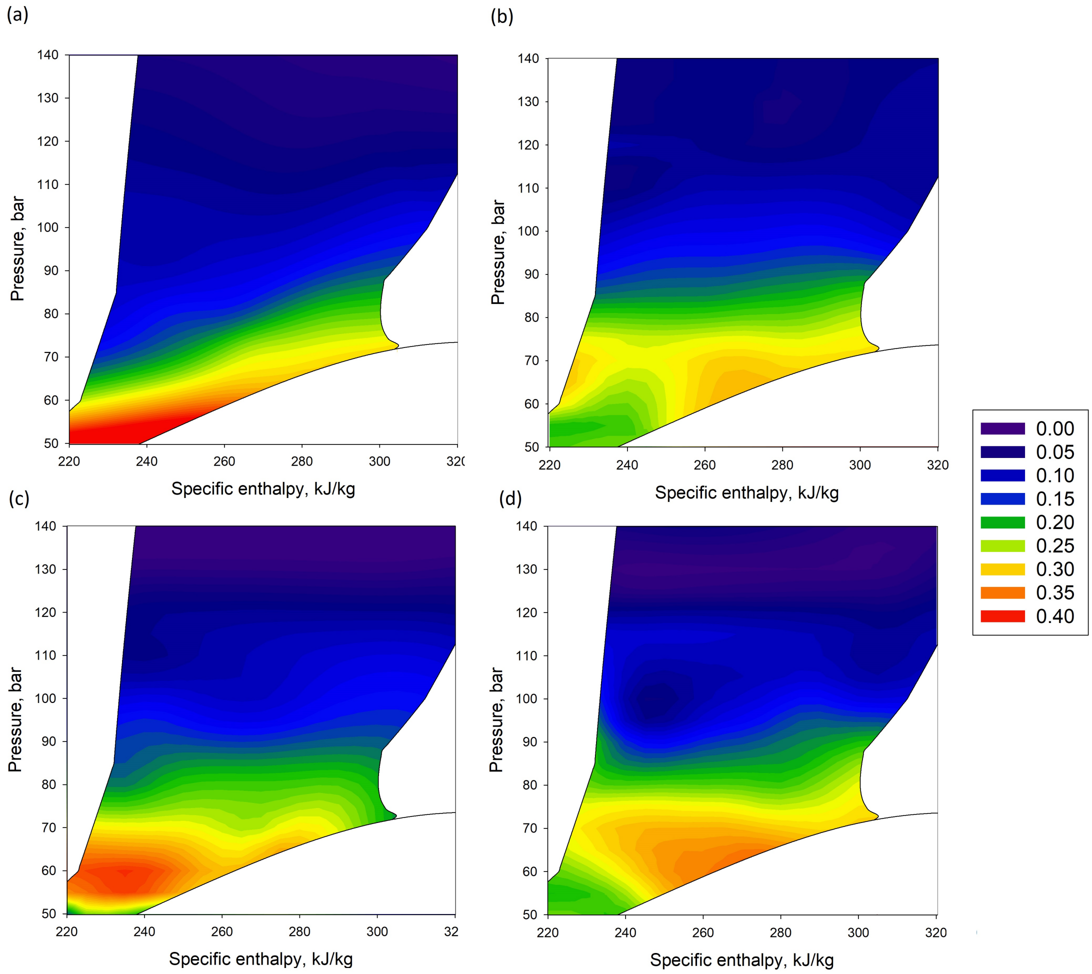


Figure 5: The ejector efficiency mapping of the investigated R744 ejectors at the MT evaporation temperature of -10 °C with the superheat of 5 K and the pressure lift of 4 bar: (a) EJ 1; (b) EJ 2; (c) EJ 3; (d) EJ 4.

approximately 37 °C. Therefore, the high performance of EJ 1 for the ambient temperature above 25 °C permitted the use of EJ 1 at high pressure lift and reduced the pressure ratio in the parallel compressors via pre-compression of the working fluid in the multi-ejector module. A similar profile of $\chi$ values was obtained in EJ 2 in Figure 7(b). Moreover, the maximum $\chi$ value of EJ 2 was much higher for pressure lift below 4 bar and ambient temperatures in the range from 25 °C to 35 °C. $\chi$ values above 0.3 were obtained at ambient temperatures in the range from 15 °C to 50 °C at different pressure lift ranges. The $\chi$ values of EJ 3 shown in Figure 7(c) were smaller than those obtained for EJ 2. However, the maximum value of $\chi$ was of approximately 0.7, which resulted in high performance of EJ 3 at the specified pressure lift. In addition, $\chi$ values above 0.3 was obtained by EJ 3 for ambient temperatures in the range from 20 °C to 46 °C. For an ambient temperature of approximately 37 °C, EJ 3 reached $\chi$ of 0.3 for the pressure lift of approximately 10 bar that was similar to results obtained for EJ 1 and EJ 2. The last ejector EJ 4 presented in Figure 7(d) achieved the highest value of $\chi$, approximately 0.8, for ambient temperatures in the range from 30 °C to 37 °C. Therefore, EJ 4 was able to entrain the suction stream from the MT evaporator at very high efficiency for ambient temperatures in the range from 15 °C to 50 °C at different pressure lift. Moreover, the $\chi$ value of 0.3 was obtained by EJ 4 for the pressure lift of approximately 12 bar and an ambient temperature of approximately 42 °C. Each investigated ejector reached high performance of the entrainment possibilities for ambient temperatures above



This is the accepted version of an article published in Energy.
DOI: 10.1016/j.energy.2018.04.088

15 °C. Hence, the $CO_2$ multi-ejector module was able to improve the energy performance of both the refrigeration system and the heat pump system at the specified temperature of outdoor air in the refrigeration system or hot water in the heat pump system. The set of high pressure lift for the refrigeration application in the HVAC&R for high ambient temperature reduced the pressure ratio in the compressors section, which influenced the total power consumption reduction and an increase of COP. In addition, the high mass entrainment ratio at specified pressure lift let to recover some potentially work during the expansion process and improve COP. Hence, a selection of pressure lift and number of running ejectors at specified cooling demand leads high efficiency of the multi-ejector module.

In addition to evaluating the application range of the R744 fixed-geometry ejectors in the refrigeration and heat pump systems, the performance of the ejectors installed in the multi-ejector module for the air-conditioning application was investigated. The most important information for utilising the multi-ejector section at high efficiency in AC mode is the proper set of pressure lift values for the different ambient temperatures to maintain high performance of the ejector and improve the energy performance of the system. Hence, the results presented in Figure 8 define the pressure lift in terms of the ambient temperature in the range from 22 °C to 50 °C based on the hybrid ROM of each investigated ejector. In addition, a cubic polynomial approximation function was introduced. Similar to the results presented in Figure 7, the motive nozzle conditions were defined based on the correlations presented by Gullo et al. [21] to obtain the best gas cooler performance at the specified ambient temperature. The suction nozzle conditions were defined for the AC evaporation temperature of 5 °C at the saturation line. As shown in Figure 8(a), the pressure lift for EJ 1 varied from 6 bar to 14 bar for ambient temperatures below 30 °C and rapidly increased to 14 bar for ambient temperatures between 30 °C and 35 °C. With further increases in the ambient temperature, the pressure lift was maintained at 14 bar, and above approximately 47 °C, the pressure lift decreased to 12 bar. For EJ 2, as shown in Figure 8(b), the pressure lift slightly increased from 6 bar to 10 bar at ambient temperatures of 33 °C and 50 °C, respectively. Although the shapes of the approximation function differed between EJ 1 and EJ 2, both ejectors exhibited the best performance for pressure lifts below 8 bar at ambient temperatures below approximately 30 °C and higher pressure lifts above 30 °C. The pressure lift of EJ 3, as shown in Figure 8(c), was below 8 bar at ambient temperatures below approximately 35 °C and above approximately 47 °C. The highest pressure lift was obtained by EJ 3 for ambient temperatures in the range from 40 °C to 46 °C. For the largest ejector, EJ 4, as shown in Figure Figure 8(d), exhibited a rapid drop from 11 bar to 6 bar for ambient temperatures in the range from 46 °C to 50 °C. The pressure lift was in the range from 6 bar to 8 bar for ambient temperatures below 35 °C. Compared to the other investigated ejectors, EJ 4 obtained similar pressure ranges. A smaller pressure lift should be defined for ambient temperatures below 35 °C and above approximately 46 °C,

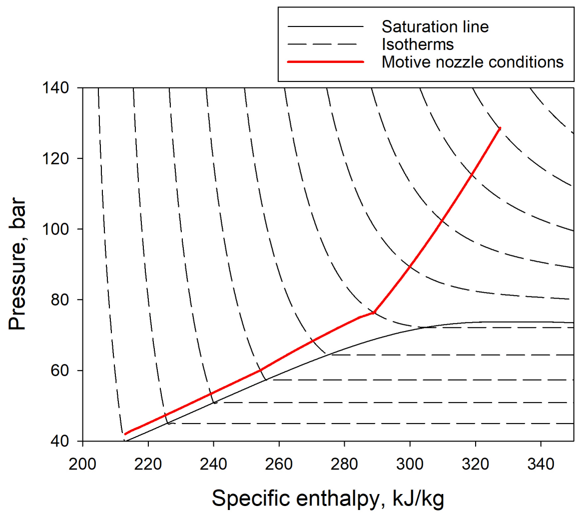


Figure 6: The R744 pressure-specific enthalpy diagram with the motive nozzle conditions based on the correlation presented by Gullo et al. [21].



This is the accepted version of an article published in Energy.
DOI: 10.1016/j.energy.2018.04.088

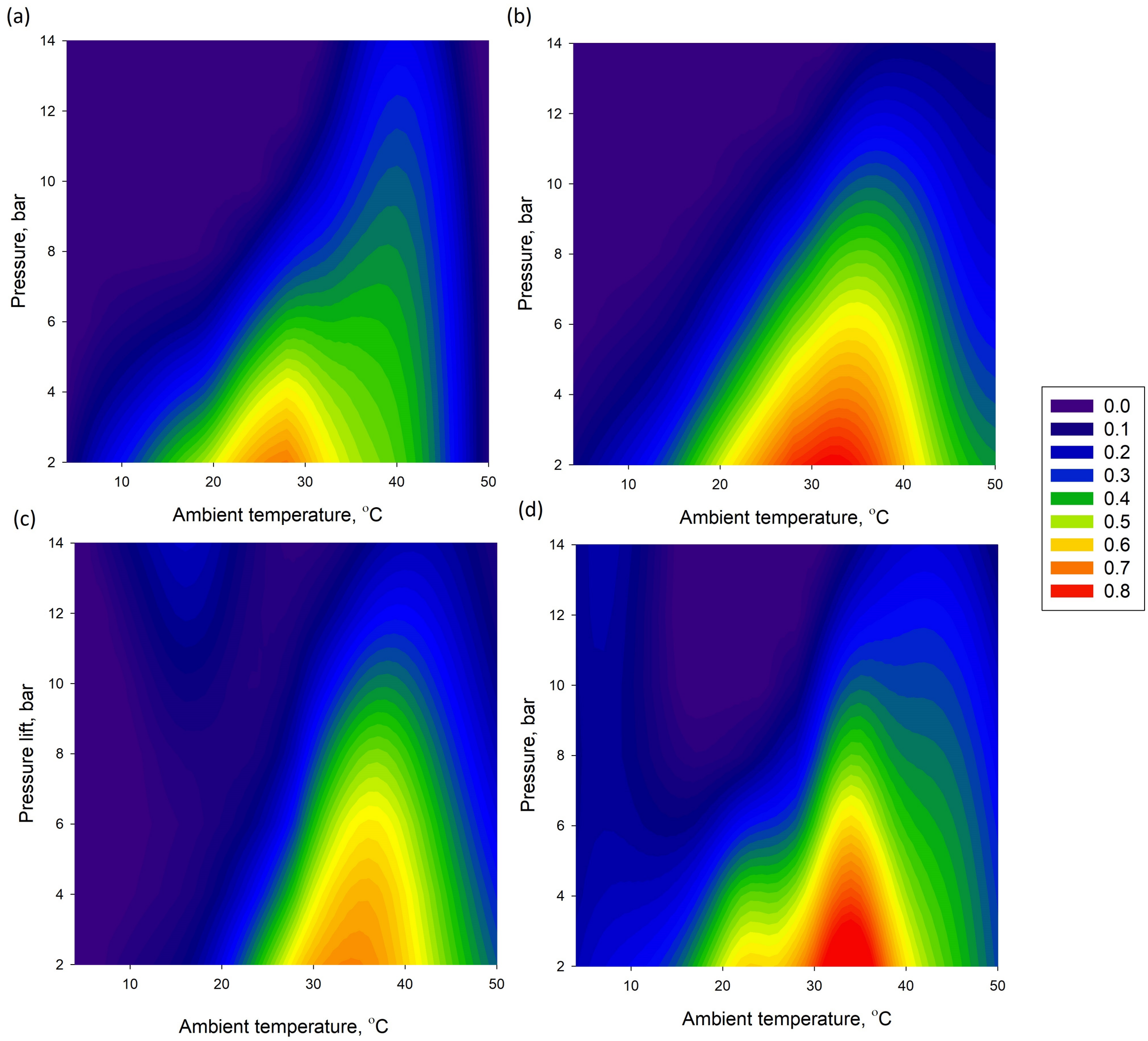


Figure 7: The mass entrainment ratio of the investigated R744 ejectors at MT evaporation temperature of -4°C for various ambient temperature and the pressure lift: (a) EJ 1; (b) EJ 2; (c) EJ 3; (d) EJ 4.

whereas a high pressure lift of 10 bar is needed for ambient temperature between 40 °C and 45 °C.

The operating curves of each investigated ejector for air-conditioning application in HVAC&R presented in Figure 8 allow the utilisation of the multi-ejector module at the best efficiency under the different ambient conditions. It can be seen that the ambient temperature below 30 °C corresponded to the pressure lift below 9 bar as the motive nozzle conditions were in subcritical region. In transcritical conditions, the pressure lift varied between 8 bar and 15 bar and the highest pressure lift occurred for the ambient temperature of approximately 45 °C. The similar pressure ranges for the different ambient temperature ranges enabled the use of the same pressure lift of the multi-ejector module during utilisation in the parallel mode. The proper selection of the multi-ejector operating conditions for air-conditioning application let to reduce the pressure ratio of the parallel compressors, which strongly related to the electric power consumption, and obtain the best possibility of the expansion work recovery inside the multi-ejector.

Based on the hybrid ROM results for each investigated ejector, the approximation functions of the pressure lift in terms of the ambient temperature were generated to obtain the best performance of the ejector for AC operating conditions, as presented in Figure 8. The coefficients of the ejector polynomial functions are shown



This is the accepted version of an article published in Energy.
DOI: 10.1016/j.energy.2018.04.088

in Table 4. Moreover, the $R^2$ values of each ejector approximation function are introduced. The $R^2$ were above 0.9, and thus the approximation functions were generated with small error compared to the hybrid ROM results. The approximation can be used in the controller system to utilise the multi-ejector system at high efficiency. The combination of the running ejectors at specified cooling demand can be selected at defined pressure lift given by the approximation function. Moreover, the high value of the pressure lift enabled the reduction of the pressure ratio in the parallel compressors, resulting in a reduction of the electric power consumption reduction and the improved system energy performance.

## 5. Conclusions

Performance mapping of the four $CO_2$ fixed-geometry ejectors installed in the multi-ejector module was performed. The results were obtained at a wide range of operating conditions to encompass the work of the ejectors in an R744 HVAC&R supermarket system. The investigation was performed based on the hybrid ROM of each investigated ejector. The hybrid ROMs were generated based on the CFD results and the experimental data. Moreover, the operational envelope of the hybrid ROM was defined to cover a wide operating regime in the $CO_2$ supermarket system at various ambient temperatures.

The validation procedure of the hybrid ROM confirmed that the reduced model of each ejector predicted the motive nozzle MFR with satisfactory accuracy within ±1% for all investigated points. Similar high accuracies of the suction nozzle MFR were obtained by the hybrid ROM based on the CFD results and the experimental data.

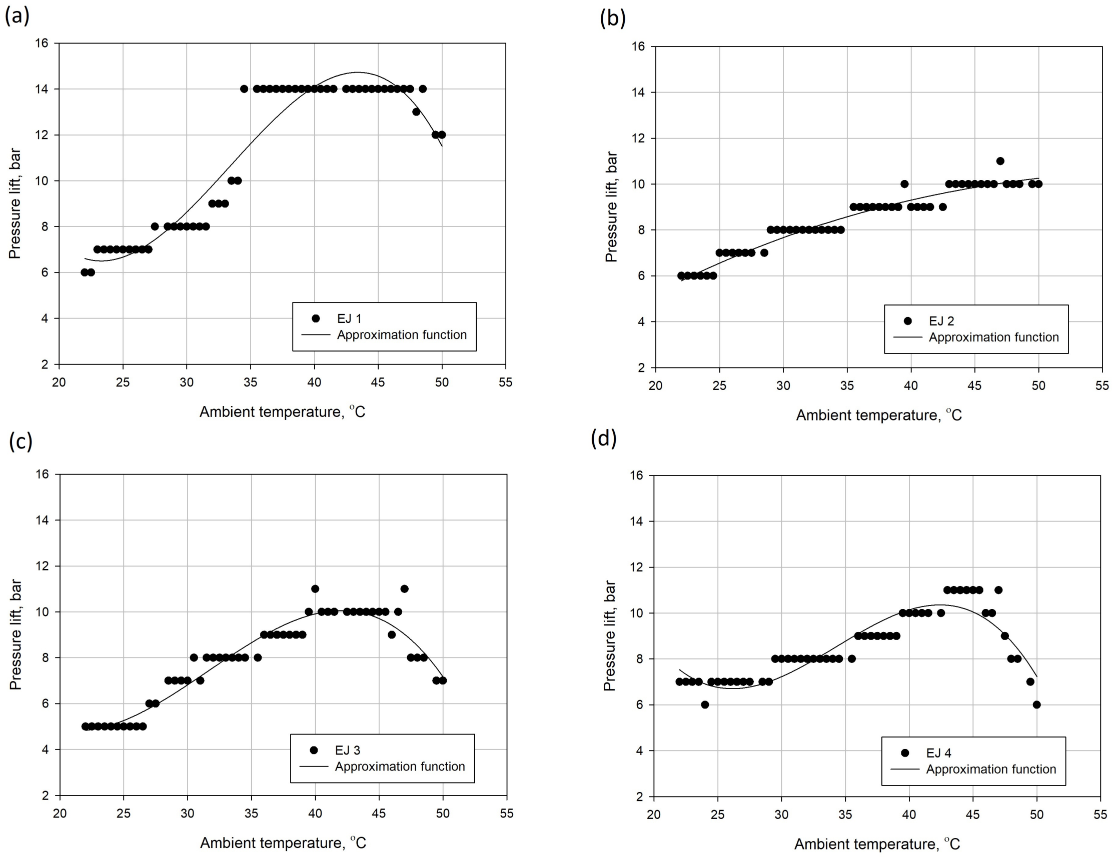


Figure 8: The pressure lift of the investigated R744 ejectors at an air-conditioning evaporation temperature of 5°C in terms of the ambient temperature for the best ejector efficiency: (a) EJ 1; (b) EJ 2; (c) EJ 3; (d) EJ 4.



This is the accepted version of an article published in Energy.
DOI: 10.1016/j.energy.2018.04.088

Table 4: The set of the approximation function coefficients for the pressure lift calculations of the investigated $CO_2$ ejectors installed in the multi-ejector module at an air-conditioning evaporation temperature of 5°C in terms of the ambient temperature for the best ejector efficiency.

$$\Delta p\,(t_{amb}) = \Delta p_0 + a \cdot t_{amb} + b \cdot t_{amb}^2 + c \cdot t_{amb}^3$$

| Ejector | $\Delta p_0$ | a | b | c | $R^2$ |
|---|---|---|---|---|---|
| EJ 1 | 64.973 | -6.1152 | 2.0175e-01 | -2.0166e-03 | 0.963 |
| EJ 2 | -2.5377 | 0.49719 | -5.8370e-03 | 2.0238e-05 | 0.944 |
| EJ 3 | 32.43 | -3.1252 | 1.1070e-01 | -1.1660e-03 | 0.963 |
| EJ 4 | 65.083 | -5.6243 | 1.7397e-01 | -1.6925e-03 | 0.914 |

Therefore, the hybrid ROM was used to analyse the performance of the R744 fixed-geometry ejectors under the typical operating conditions for refrigeration, air-conditioning and heat pump applications.

The motive nozzle MFR mapping was performed for each ejector to define the ejector capacity at different gas cooler outlet conditions. The motive nozzle pressure was in the range from 50 bar to 140 bar according to the specified hybrid ROM operational envelope. All ejectors exhibited similar trends of increasing motive nozzle MFR. A small difference was observed for EJ 4 for motive nozzle pressures between 80 and 100 bar. Each of the investigated ejectors obtained the highest value of the motive nozzle MFR at a pressure of 140 bar and specific enthalpy of approximately 220 kJ/kg and the lowest value of the motive nozzle pressure at 50 bar.

The ejector efficiency mapping of the ejectors installed in the $CO_2$ multi-ejector module indicated the area of high ejector efficiency for different motive nozzle conditions. The suction nozzle pressure was 26 bar with a superheat of 5 K and a pressure lift of 4 bar. Each ejector obtained the best performance for the motive nozzle pressure in the range from 60 bar to 90 bar. However, satisfactory ejector efficiency from 0.2 to 0.3 was achieved by all investigated ejectors in the pressure range between 50 bar and approximately 100 bar and above 0.3 in the sub-critical region. Therefore, the multi-ejector module at different gas cooler outlet conditions was able to maintain high performance in either single-operation mode or parallel mode as the result of the performance of the individual ejectors.

The mass entrainment ratio was investigated to evaluate the influence of the ambient temperature and pressure lift on the entrainment possibilities of each ejector. The motive nozzle conditions were defined to reach the best performance of the gas cooler at the specified ambient temperature, and the suction nozzle conditions were set based on the MT evaporation temperature of -4 °C. In addition, the suction stream was defined as the saturated vapour resulting from the MT evaporator flooded operation mode. A mass entrainment ratio above 0.3 was obtained for ambient temperatures in the range from 15 °C to approximately 50 °C for all investigated $CO_2$ ejectors. Moreover, a high mass entrainment ratio was obtained for high values of the pressure lift up to 10 bar at an ambient temperature of approximately 37 °C for EJ 1, EJ 2 and EJ 3 and up to 12 bar at a temperature of approximately 42 °C. Hence, the high entrainment possibilities together with the high pressure difference between the outlet and suction nozzles enabled the efficient use of the fixed-geometry ejectors, which strongly influenced the multi-ejector performance and the energy performance of the R744 supermarket refrigeration system.

The performance of the investigated $CO_2$ ejectors for the air-conditioning application at different ambient temperatures was evaluated to define the best value of pressure lift at a specified ambient temperature in the range from 22 °C to 50 °C. In addition, a cubic polynomial approximation function was proposed for each ejector. The investigated R744 fixed-geometry ejectors obtained the best performance for pressure lift in the range from approximately 6 bar to 14 bar. The high value of the pressure lift together with the high efficiency of each ejector enabled the utilisation of the multi ejector equipped with the investigated ejectors at similar efficiency either in single operating mode or parallel mode. Hence, multi-ejector performance should be evaluated based on the proposed hybrid ROMs of the ejectors to analyse the energy performance improvement of $CO_2$ multi-ejector HVAC&R systems for supermarkets.



This is the accepted version of an article published in Energy.
DOI: 10.1016/j.energy.2018.04.088

## 6. Acknowledgement

The authors gratefully acknowledge the financial support of the Research Council of Norway through project No. 244009/E20. The work of MH was also partially supported by the Rector's research grant No. 08/060/RGJ18/0157 provided by SUT.

## References

[1] U. N. E. Programme, O. Secretariat, Handbook for the montreal protocol on substances that deplete the ozone layer.
[2] M. H. Kim, J. Pettersen, C. W. Bullard, Fundamental process and system design issues in $CO_2$ vapor compression systems, Progress in Energy and Combustion Science 30 (2) (2004) 119–174. doi:10.1016/j.pecs.2003.09.002.
[3] V. Sharma, B. Fricke, P. Bansal, Comparative analysis of various $CO_2$ configurations in supermarket refrigeration systems, International Journal of Refrigeration-Revue Internationale Du Froid 46 (2014) 86–99. doi:DOI10.1016/j.ijrefrig.2014.07.001.
[4] P. Gullo, B. Elmegaard, G. Cortella, Advanced exergy analysis of a R744 booster refrigeration system with parallel compression, Energy 107 (2016) 562 – 571. doi:https://doi.org/10.1016/j.energy.2016.04.043.
[5] S. Elbel, P. Hrnjak, Flash gas bypass for improving the performance of transcritical R744 systems that use microchannel evaporators, International Journal of Refrigeration-Revue Internationale Du Froid 27 (7) (2004) 724–735. doi:DOI10.1016/j.ijrefrig.2004.07.019.
[6] G. Besagni, R. Mereu, F. Inzoli, Ejector refrigeration: A comprehensive review, Renewable and Sustainable Energy Reviews 53 (Supplement C) (2016) 373 – 407. doi:https://doi.org/10.1016/j.rser.2015.08.059.
[7] J. Sarkar, Optimization of ejector-expansion transcritical $CO_2$ heat pump cycle, Energy 33 (9) (2008) 1399 – 1406. doi:https://doi.org/10.1016/j.energy.2008.04.007.
[8] X. X. Xu, G. M. Chen, L. M. Tang, Z. J. Zhu, Experimental investigation on performance of transcritical $CO_2$ heat pump system with ejector under optimum high-side pressure, Energy 44 (1) (2012) 870 – 877, integration and Energy System Engineering, European Symposium on Computer-Aided Process Engineering 2011. doi:https://doi.org/10.1016/j.energy.2012.04.062.
[9] S. Elbel, P. Hrnjak, Experimental validation of a prototype ejector designed to reduce throttling losses encountered in transcritical R744 system operation, International Journal of Refrigeration-Revue Internationale Du Froid 31 (3) (2008) 411–422. doi:DOI10.1016/j.ijrefrig.2007.07.013.
[10] M. Haida, J. Smolka, M. Palacz, J. Bodys, A. J. Nowak, Z. Bulinski, A. Fic, A. Hafner, K. Banasiak, A. Hafner, Numerical investigation of an R744 liquid ejector for supermarket refrigeration systems, Thermal Science 20 (4) (2016) 1259–1269.
[11] F. Liu, E. A. Groll, D. Li, Investigation on performance of variable geometry ejectors for $CO_2$ refrigeration cycles, Energy 45 (1) (2012) 829 – 839. doi:https://doi.org/10.1016/j.energy.2012.07.008.
[12] Y. He, J. Deng, F. Yang, Z. Zhang, An optimal multivariable controller for transcritical $CO_2$ refrigeration cycle with an adjustable ejector, Energy Conversion and Management 142 (Supplement C) (2017) 466 – 476. doi:https://doi.org/10.1016/j.enconman.2017.03.070.
[13] Y. He, J. Deng, L. Zheng, Z. Zhang, Performance optimization of a transcritical $CO_2$ refrigeration system using a controlled ejector, International Journal of Refrigeration 75 (Supplement C) (2017) 250 – 261. doi:https://doi.org/10.1016/j.ijrefrig.2016.12.015.
[14] A. Hafner, S. Forsterling, K. Banasiak, Multi-ejector concept for R-744 supermarket refrigeration, International Journal of Refrigeration-Revue Internationale Du Froid 43 (2014) 1–13. doi:DOI10.1016/j.ijrefrig.2013.10.015.
[15] K. Banasiak, A. Hafner, E. E. Kriezi, K. B. Madsen, M. Birkelund, K. Fredslund, R. Olsson, Development and performance mapping of a multi-ejector expansion work recovery pack for R744 vapour compression units, International Journal of Refrigeration 57 (2015) 265–276. doi:http://dx.doi.org/10.1016/j.ijrefrig.2015.05.016.
[16] M. Haida, K. Banasiak, J. Smolka, A. Hafner, T. M. Eikevik, Experimental analysis of the R744 vapour compression rack equipped with the multi-ejector expansion work recovery module, International Journal of Refrigeration 64 (2016) 93–107. doi:10.1016/j.ijrefrig.2016.01.017.
[17] G. Boccardi, F. Botticella, G. Lillo, R. Mastrullo, A. Mauro, R. Trinchieri, Thermodynamic Analysis of a Multi-Ejector, $CO_2$, Air-To-Water Heat Pump System, Energy Procedia 101 (Supplement C) (2016) 846 – 853, aTI 2016 - 71st Conference of the Italian Thermal Machines Engineering Association. doi:https://doi.org/10.1016/j.egypro.2016.11.107.
[18] G. Boccardi, F. Botticella, G. Lillo, R. Mastrullo, A. Mauro, R. Trinchieri, Experimental investigation on the performance of a transcritical $CO_2$ heat pump with multi-ejector expansion system, International Journal of Refrigeration 82 (Supplement C) (2017) 389 – 400. doi:https://doi.org/10.1016/j.ijrefrig.2017.06.013.
[19] L. Cecchinato, M. Corradi, S. Minetto, Energy performance of supermarket refrigeration and air conditioning integrated systems, Applied Thermal Engineering 30 (14) (2010) 1946 – 1958. doi:https://doi.org/10.1016/j.applthermaleng.2010.04.019.
[20] M. Karampour, S. Sawalha, State-of-the-art integrated co2 refrigeration system for supermarkets: A comparative analysis, International Journal of Refrigeration 86 (2018) 239 – 257.
[21] P. Gullo, A. Hafner, G. Cortella, Multi-ejector R744 booster refrigerating plant and air conditioning system integration – a theoretical evaluation of energy benefits for supermarket applications, International Journal of Refrigeration 75 (2017) 164– 176. doi:http://dx.doi.org/10.1016/j.ijrefrig.2016.12.009.
[22] A. Kornhauser, The use of an ejector as a refrigerant expander, in: International Refrigeration and Air Conditioning Conference, Purdue University, Purdue ePubs, The address of the publisher, 1990, pp. 1–11, an optional note.
[23] C. Richter, Proposal of new object-oriented equation-based model libraries for thermodynamic systems, Ph.D. thesis, Braunschweig University of Technology (2008).
[24] S. Elbel, N. Lawrence, Review of recent developments in advanced ejector technology, International Journal of Refrigeration 62 (2016) 1–18. doi:http://dx.doi.org/10.1016/j.ijrefrig.2015.10.031.



This is the accepted version of an article published in Energy.
DOI: 10.1016/j.energy.2018.04.088

[25] J. Smolka, Z. Bulinski, A. Fic, A. J. Nowak, K. Banasiak, A. Hafner, A computational model of a transcritical R744 ejector based on a homogeneous real fluid approach, Applied Mathematical Modelling 37 (3) (2013) 1208–1224. doi:http://dx.doi.org/10.1016/j.apm.2012.03.044.
[26] E. W. Lemmon, M. L. Huber, M. O. McLinden, NIST Standard Reference Database 23: Reference Fluid Thermodynamic and Transport Properties - REFPROP, National Institute of Standards and Technology, Standard Reference Data Program.
[27] M. Palacz, J. Smolka, A. Fic, Z. Bulinski, A. J. Nowak, K. Banasiak, A. Hafner, Application range of the hem approach for co2 expansion inside two-phase ejectors for supermarket refrigeration systems, International Journal of Refrigeration 59 (2015) 251 – 258.
[28] M. Haida, J. Smolka, A. Hafner, M. Palacz, K. Banasiak, A. J. Nowak, Modified homogeneous relaxation model for the R744 trans-critical flow in a two-phase ejector, International Journal of Refrigeration 85 (2018) 314 – 333.
[29] C. A. Rogers, A. J. Kassab, E. A. Divo, Z. Ostrowski, R. A. Bialecki, An inverse POD-RBF network approach to parameter estimation in mechanics, Inverse Problems in Science and Engineering 20 (5) (2012) 749–767. doi:10.1080/17415977.2012.693080.
[30] G. Węcel, Z. Ostrowski, P. Kozołub, Absorption line black body distribution function evaluated with proper orthogonal decomposition for mixture pf $CO_2$ and $H_20$, International Journal of Numerical Methods for Heat and Fluid Flow 24 (4) (2014) 932–948. doi:http://dx.doi.org/10.1108/HFF-04-2013-0142.
[31] M. Haida, J. Smolka, A. Hafner, Z. Ostrowski, M. Palacz, A. J. Nowak, K. Banasiak, System model derivation of the $CO_2$ two-phase ejector based on the cfd-based reduced-order model, Energy 144 (2018) 941 – 956. doi:https://doi.org/10.1016/j.energy.2017.12.055.
[32] Z. Ostrowski, R. A. Białecki, A. J. Kassab, Solving inverse heat conduction problems using trained POD-RBF network inverse method, Inverse Problems in Science and Engineering 16 (1) (2008) 39–54. doi:10.1080/17415970701198290.
[33] G. H. Golub, C. F. Van Loan, Matrix computation, The Johns Hopkins University Press, 1996.
[34] A. Fluent, Ansys fluent user's guide, PA, Canonsburg.
[35] F. Mazzelli, A. B. Little, S. Garimella, Y. Bartosiewicz, Computational and experimental analysis of supersonic air ejector: Turbulence modeling and assessment of 3d effects, International Journal of Heat and Fluid Flow 56 (2015) 305 – 316.
[36] M. Palacz, J. Smolka, W. Kus, A. Fic, Z. Bulinski, A. J. Nowak, K. Banasiak, A. Hafner, CFD-based shape optimisation of a $CO_2$ two-phase ejector mixing section, Applied Thermal Engineering 95 (2016) 62–69.
[37] K. Banasiak, A. Hafner, Mathematical modelling of supersonic two-phase R744 flows through converging–diverging nozzles: The effects of phase transition models, Applied Thermal Engineering 51 (1–2) (2013) 635 – 643. doi:http://dx.doi.org/10.1016/j.applthermaleng.2012.10.005.
[38] J. Bodys, J. Smolka, M. Palacz, M. Haida, K. Banasiak, A. J. Nowak, A. Hafner, Performance of fixed geometry ejectors with a swirl motion installed in a multi-ejector module of a $CO_2$ refrigeration system, Energy 117 (Part 2) (2016) 620 – 631, the 28th International Conference on Efficiency, Cost, Optimization, Simulation and Environmental Impact of Energy Systems - ECOS 2015. doi:https://doi.org/10.1016/j.energy.2016.07.037.
[39] M. Palacz, J. Smolka, A. J. Nowak, K. Banasiak, A. Hafner, Shape optimisation of a two-phase ejector for $CO_2$ refrigeration systems, International Journal of Refrigeration 74 (2017) 210–221. doi:http://dx.doi.org/10.1016/j.ijrefrig.2016.10.013.
[40] J. Bodys, M. Palacz, M. Haida, J. Smolka, A. J. Nowak, K. Banasiak, A. Hafner, Full-scale multi-ejector module for a carbon dioxide supermarket refrigeration system: Numerical study of performance evaluation, Energy Conversion and Management 138 (2017) 312 – 326. doi:http://dx.doi.org/10.1016/j.enconman.2017.02.007.



This is the accepted version of an article published in Energy.
DOI: 10.1016/j.energy.2018.04.088